Cell. Mol. Life Sci. (2010) 67:3557–3568
DOI 10.1007/s00018-010-0395-6

Cellular and Molecular Life Sciences

RESEARCH ARTICLE

The transcription factor EGR1 regulates metastatic potential of *v-src* transformed sarcoma cells

Vladimír Čermák · Jan Kosla · Jiří Plachý · Kateřina Trejbalová · Jiří Hejnar · Michal Dvořák

Received: 9 October 2009 / Revised: 27 April 2010 / Accepted: 29 April 2010 / Published online: 28 May 2010

Abstract Metastatic spreading of cancer cells is a highly complex process directed primarily by the interplay between tumor microenvironment, cell surface receptors, and actin cytoskeleton dynamics. To advance our understanding of metastatic cancer dissemination, we have developed a model system that is based on two *v-src* transformed chicken sarcoma cell lines—the highly metastatic parental PR9692 and a non-metastasizing but fully tumorigenic clonal derivative PR9692-E9. Oligonucleotide microarray analysis of both cell lines revealed that the gene encoding the transcription factor EGR1 was downregulated in the non-metastatic PR9692-E9 cells. Further investigation demonstrated that the introduction of exogenous EGR1 into PR9692-E9 cells restored their metastatic potential to a level indistinguishable from parental PR9692 cells. Microarray analysis of EGR1 reconstituted cells revealed the activation of genes that are crucial for actin cytoskeleton contractility (MYL9), filopodia formation (MYO10), the production of specific extracellular matrix components (HAS2, COL6A1-3) and other essential pro-metastatic abilities.

Keywords EGR1 · Sarcoma · Metastasis · Regulation of expression · Transcription · Microarrays

Electronic supplementary material The online version of this article (doi:10.1007/s00018-010-0395-6) contains supplementary material, which is available to authorized users.

V. Čermák · J. Kosla · J. Plachý · K. Trejbalová · J. Hejnar · M. Dvořák (✉)
Institute of Molecular Genetics AS CR, v.v.i. Vídeňská 1083, 142 20 Prague, Czech Republic
e-mail: mdvorak@img.cas.cz

Introduction

Metastatic dissemination of malignant tumors is the most severe and usually fatal complication of cancer. Despite substantial progress in the field of cancer metastasis research, our understanding of this process is far from complete, although it is generally accepted that extracellular matrix (ECM) degrading proteases, actin cytoskeleton dynamics, and specific adhesion receptors are involved [1–3]. For an individual tumor to become metastatic, a number of gene expression requirements are likely to be met and are determined by cell type, the accumulation of genetic and epigenetic changes acquired during the transformation process, as well as the specific microenvironment within the tumor cell mass [4]. In carcinomas (tumors derived from epithelial cells), it is known that the critical step for metastatic progression is the transient switch of tumor cells from an epithelial phenotype to a mesenchymal-like one. This process is called the epithelial-mesenchymal transition (EMT) [5, 6] and is responsible for releasing the carcinoma cell from adherens junctions through repressing the expression of E-cadherin. In addition, mesenchymal specific gene expression is also likely to provide a cancer cell with migratory abilities in ECM. According to this hypothesis, one would expect that tumors derived from mesenchymal cells (sarcomas), would easily disseminate. However, this is not always the case, as, for example, only approximately 20% of human extremity soft tissue sarcomas proceed to the metastatic stage [7, 8]. Similarly, we have observed in our CC.R1 chicken animal model that *v-src* induced fibrosarcomas are non-metastasizing (unpublished observation). Given these observations, it is obvious that the mesenchymal phenotype itself is not sufficient to endow a transformed cell with metastatic abilities. Therefore, an additional level of transcriptional regulation must exist that is responsible for

the expression of metastasis-promoting genes. Understanding this regulation will be critical for better metastasis management in sarcoma as well as carcinoma patients.

In an effort to extend our knowledge of genes involved in controlling the metastatic behavior of mesenchymal cancer cells, we developed an experimental model based on two *v-src* transformed chicken fibrosarcoma cell lines—the highly metastatic parental PR9692 cells and the non-metastasizing clone, PR9692-E9. Upon inoculation into the pectoral muscle of experimental animals, both cell lines form rapidly growing primary tumors, but only the parental PR9692 cells give rise to lung metastases. There are also substantial differences in the morphology and behavior of these cells under tissue culture conditions, namely in their adhesive properties. To gain insight into the molecular background of the different metastatic behavior of these cell lines, we performed a gene expression analysis using oligonucleotide microarrays. The analysis revealed a number of genes that were differentially expressed in the non-metastatic PR9692-E9 cells compared to parental cells, including the transcriptional regulator EGR1 that showed a 20-fold downregulation. EGR1 is a member of the EGR family of immediate early genes whose expression is under the direct control of MAPK signaling. As such, EGR proteins regulate the cellular response to various extracellular cues, with their target genes being highly cell-type specific. The target genes of EGR1 in mesenchymal cells published so far include ID1 [9], ID2 [10], THBS1 [11], TNC [12], COL1A2 [13], and PDGFA [14]. Importantly, EGR1 has been shown to participate in mediating TGFβ signaling [13, 15], which is known to affect metastatic behavior of cancer cells [16]. To elucidate whether the loss of metastatic potential in PR9692-E9 cells is a result of the decrease in EGR1 expression we established PR9692-E9-EGR1 cells that express EGR1 from a non-replicating integrated retroviral vector. Inoculation of these cells into experimental animals revealed a full restoration of metastatic potential. To determine the changes in gene expression following exogenous EGR1 expression, an oligonucleotide microarray analysis was performed. By comparing the gene expression profiles of all three cell lines we have revealed a number of potential EGR1 target genes that may be involved in metastatic spreading and include regulators of actin cytoskeleton contractility, filopodia formation, ECM production, and matrix metalloproteinase activation.

Materials and methods

DNA constructs

The ΛF6K4cl2 phage DNA used for the induction of the original tumor was constructed by Svoboda et al. [17]. SFCV-ME-EGR1 was constructed by introducing the full-length chicken EGR1 cDNA (GenBank accession number AY034140) together with the 5′-terminaly added myc epitope (AEEQKLISEEDLL) between Hind III and Xba I sites of the SFCV-LE vector [18].

Animals

Experiments were done with the Prague inbred chicken line CC.R1 [19]. All procedures were performed in accordance with the Guide for the Care and Use of Laboratory Animals and approved by the Animal Care and Use Committee of the Academy of Sciences of the Czech Republic. Chicks were kept under standard laboratory conditions with free access to food and water.

Establishment of stable cell lines

The cell line PR9692 was derived from a tumor that arose after injection of a ΛF6K4cl2 DNA construct that contained *v-src* cDNA between RSV LTR sequences ("LTR, *v-src*, LTR") into the outer area of pectoral muscle of an experimental chick No. 9692 [20]. Tissue fragments of a tumor from a chick transplanted with the original tumor No. 9692 were then transferred into cell culture and the cells were passaged until they spontaneously immortalized. The PR9692 tumor cells have now been in continuous culture for over 10 years (more than 500 population doublings (PDs) over 200 serial passages). The cells grow at a constant proliferation rate (PD time 20–25 h) and are clonogenic (colony-forming efficiency approximately 50%). Clone PR9692-E9 was derived by performing a limiting dilution of the PR9692 cells at in vitro passage 175. PR9692 and all the derived cell lines were grown in Iscove's modified Dulbecco's minimal essential medium supplemented with 8% fetal calf serum, 2% chicken serum, and antibiotics. The cells were cultured at 40°C in a humidified atmosphere with 5% CO_2. PR9692-E9-EGR1 cells were derived from PR9692-E9 cells by infection of the cells in culture with retroviral particles that were formed after transfecting KUNDRA packaging cells with the SFCV-ME-EGR1 plasmid. Several tens of clones were obtained after G418 selection (500 μg/ml). These clones were pooled and further passaged under the conditions described above. Empty SFCV-LE vector infected control cell line designated PR9692-E9-mock was prepared in the same way. KUNDRA cells, an envC variant of the cell line described in [21], were grown in DMEM supplemented with glutamine, antibiotics, 4% fetal calf serum, and 2% chicken serum. The transfection was performed using Lipofectamine 2000 (Invitrogen) according to the manufacturer's instructions.

Monitoring of tumor growth and metastases

Chickens were inoculated by injection into the outer area of pectoral muscle at 6 weeks of age with 10^5 tumor cells that were freshly harvested from the tissue culture and resuspended in 0.2 ml of cultivation medium. The area of the primary tumor present at the pectoral muscle was measured by placing transparent foil on the tumor and tracing its contours. The contour lines were then transferred onto a sheet of millimeter paper and tumor area (mm^2) calculated [20]. Growth rates of tumors induced by different cell types were statistically evaluated by one-way ANOVA in Excel (Microsoft). The spontaneous metastatic activity of each tumor cell line was determined by examining autopsied chickens 5 weeks after inoculation. Metastases were observed by gross inspection and using a dissection microscope. The experiments were performed several times with a total number of approximately 50 animals in each group except the PR9692-E9-mock group where the numbers were reduced to spare animals.

RNA preparation, reverse transcription, PCR, qPCR

Approximately 10 million cells were harvested and RNA was extracted by immediately dissolving the cell pellet in 2 ml of Trizol reagent (Invitrogen) following the manufacturer's instructions. cDNA was prepared from 1.5 μg of total RNA using 200 U of M-MLV reverse transcriptase (Promega) in a final volume of 15 μl. The resulting product was diluted to 70 μl with PCR-grade water and used for PCR and quantitative PCR (qPCR). PCR was performed with Taq DNA polymerase (New England Biolabs) and the resulting products were resolved on a 1.3% agarose gel. For qPCR, each sample was prepared in triplicate by placing 1 μl of cDNA template with the LightCycler® 480 SYBR Green I Master mix (Roche) to a final volume of 15 μl. Samples were amplified in the Chromo 4 device (Bio-Rad). Each cell line was represented by three independent biological samples. Primer sequences and annealing temperatures can be found in Supplementary Table S4. Data analysis was performed with the aid of the Opticon Monitor software (Bio-Rad) and Excel (Microsoft). The relative abundances of mRNAs in the samples were approximated with $2^{\Delta C(t)}$ values. Significance of differences was estimated with the Welch's *t* test for pairs PR9692 vs. PR9692-E9 and PR9692-E9-EGR1 vs. PR9692-E9, respectively.

Microarray analysis and data processing

The quality and quantity of total RNA was measured on the Nanodrop spectrophotometer and Bioanalyzer capillary electrophoresis. The RNA was labeled according to the Expression Analysis Technical Manual (Affymetrix, 2001) and hybridized to the Affymetrix Genome Chicken Array. Briefly, 5 μg of total RNA was reverse transcribed into double-stranded cDNA with oligo(dT) primers tagged with a T7 promoter sequence. The double-stranded cDNA was subsequently used as a template and amplified by T7 RNA polymerase to produce many copies of antisense cRNA. Biotin-labeled nucleotides were incorporated in the cRNA during the in vitro transcription reaction. Twenty micrograms of labeled cRNA was fragmented and hybridized to the Genome Chicken Array at 45°C for 16 h. The arrays were washed and stained in the Affymetrix Fluidics Station 450 and scanned using the Affymetrix GeneChip Scanner 3000.

Raw data were normalized using the GCRMA normalization algorithm [22] and default annotation provided by Affymetrix. Only genes expressed in at least one group were used in subsequent analyses. Filtrated data were tested for differences in expression using the moderated *t* test from the limma package [23] of Bioconductor repository [24]. Raw *p* value was adjusted using the Benjamini and Hochberg method [25].

To find groups of genes with similar expression patterns in the set of samples, gene clustering was carried out with the MeV v4.3 software [26] using the QT_Clust algorithm [27]. In each row the intensities in $\log_2$ scale were subtracted with the median value of PR9692-E9 samples. The data were loaded into MeV software as "two-color chip". The variance filter was applied to restrict the analysis to 500 high SD genes. The parameters of QT_Clust algorithm were: Distance metrics—Pearson correlation, diameter 0.2, minimum cluster size 7.

Adhesion assay and phalloidin staining

To analyze the adhesive behavior of cells, 100,000 were plated on type I collagen (rat tail, Sigma C3867-1VL) coated 60-mm dishes and left to adhere overnight. Tissue culture dishes were coated according to the manufacturer's instructions. Ten fields containing approximately 300 cells each were taken by digital camera (Leica DFC420). The photographs were then analyzed visually and cells counted and divided into categories based on the degree of adhesion.

To compare the differences in actin cytoskeleton organization, the cells were plated as described above. The cells were then washed twice with phosphate buffered saline (PBS), fixed with 4% paraformaldehyde for 15 min, and stained with a 50 μg/ml solution of phalloidin-TRITC (Sigma P1951) for 40 min. Subsequently, the cells were washed twice with PBS and observed on a Leica DMI6000/TCS SP5 AOBS TANDEM confocal microscope and images taken with a Leica DFC420C digital camera.

Time-lapse microscopy

Cells (100,000) were plated on a six-well plate coated with type I collagen (rat tail, Sigma C3867-1VL) and incubated for 2 h at 40°C. Floating debris and cells that did not adhere were removed by three washes with 40°C warm culture medium. The plate was then placed in the BL109 incubator (PeCon GmbH) assembled on a Leica DMI6000B microscope, preheated to 40°C. The photographs were taken at 1-min intervals in the course of 26 h using a Leica DFC360 FX camera. Multiple positions were followed at the same time. The picture series were processed to video files in VirtualDub 1.9.8., 20 frames per second. Final compression was performed using an mpeg-2 codec.

Immunoblotting

Cells were plated on 100-mm dishes and grown until subconfluent. Before lysis, the cells were transferred into 15-ml tubes and centrifuged. The pellets were dissolved in 500 µl of LysBuf (20 mM Tris pH 6.8, 1% Triton × 100, 0.3% SDS, 5 mM EDTA, 10% glycerol, protease inhibitor cocktail Complete, EDTA-free from Roche, one tablet per 50 ml). The lysates were then sonicated for 20 s and cleared by centrifugation at 15,000 rpm for 20 min in 1.5-ml tubes. Protein concentration was assayed by the bicinchonic acid method (Pierce), the lysates were diluted to equal concentration with LysBuf, mixed with 5× SB (300 mM Tris pH 6.8, 5% SDS, 360 mM 2-mercaptoethanol, 50% glycerol, 0.05% bromphenol blue) and incubated at 99°C for 10 min. Eighty micrograms of total protein was separated on a 9% polyacrylamide gel by SDS-PAGE and transferred to a nitrocellulose membrane. The membrane was then blocked in 5% skim milk in TBST (20 mM Tris pH 7.5, 150 mM NaCl, 0.1% Tween 20). To detect EGR1, the rabbit polyclonal antibody sc-110 (Santa Cruz Biotechnology) diluted 1:2,000 in TBST with 5% skim milk (overnight incubation) and the HRP-conjugated secondary anti-rabbit antibody (Jackson ImmunoResearch Laboratories) was used. The luminescent reaction was performed using the WestDura solution (Pierce). HAS2 and NCAM1 proteins were detected using the same procedure and antibodies sc-66916, 1:2,000 (Santa Cruz Biotechnology) and 5e-a, 1:1,000 (Developmental Studies Hybridoma Bank), respectively. Equal protein loading and transfer was verified by Ponceau-S staining of the membrane and by performing immunodetection of GAPDH (GeneTex GTX30666, 1:2,000) on the same membrane.

Results

PR9692 and PR9692-E9 cell lines

To identify the genes involved in regulating the metastatic behavior of sarcoma cells, we analyzed our previously established cell lines, PR9692 and PR9692-E9. These cells were derived from a sarcoma that formed in the pectoral muscle of an experimental chick after direct injection of the cloned LTR, *v-src*, LTR DNA construct. Previous analysis established that these cells possess one copy of the LTR, v-*src*, LTR provirus and express high level of v-*src* mRNA. The integration site was identified and the maintenance of the unaltered LTR, v-*src*, LTR provirus during in vitro passaging was confirmed ([21] and unpublished results). The parental PR9692 cells adhere to uncoated cell culture plastic and display a mixed morphology of elongated and rounded cells (Fig. 1b and Supplementary Fig. S1). Upon inoculation into the pectoral muscle of experimental chicks, these cells give rise to rapidly growing sarcomas confined to sites of injection. These tumors efficiently disseminate into lungs. In contrast, PR9692-E9 cells (a subclone of PR9692 cells) grow in culture as floating aggregates with almost no adherence to uncoated plastic (Fig. 1b and Supplementary Fig. S1). Analogous to parental cells, the PR9692-E9 cells also efficiently form sarcomas in chickens however, these tumors never metastasize. Typical primary tumor growth kinetics and their metastatic characteristics are illustrated in Fig. 1a, d. There is high variability among individual animals, however, statistical analysis reveals that the tumors induced by PR9692 cells grow in average slightly faster (p value < 0.02) than those induced by PR9692-E9 cells (and their descendants).

Gene expression analysis

To elucidate any differences in gene expression that might explain the disparity between the PR9692 and PR9692-E9 cells with respect to their metastatic behavior, three independent samples of each cell line were analyzed using the Affymetrix Chicken Gene Chips. All the resulting raw data was deposited in the NCBI GEO database under the accession number GSE15141 (http://www.ncbi.nlm.nih.gov/geo/). Data analysis was performed using the Bioconductor software. Selected genes showing the most significant difference of expression level between the two cell lines are summarized in Table 1. A complete list of all genes showing at least a two-fold difference in expression is included in Supplementary Table S1. Interestingly, some of the genes downregulated in PR9692-E9 cells are known

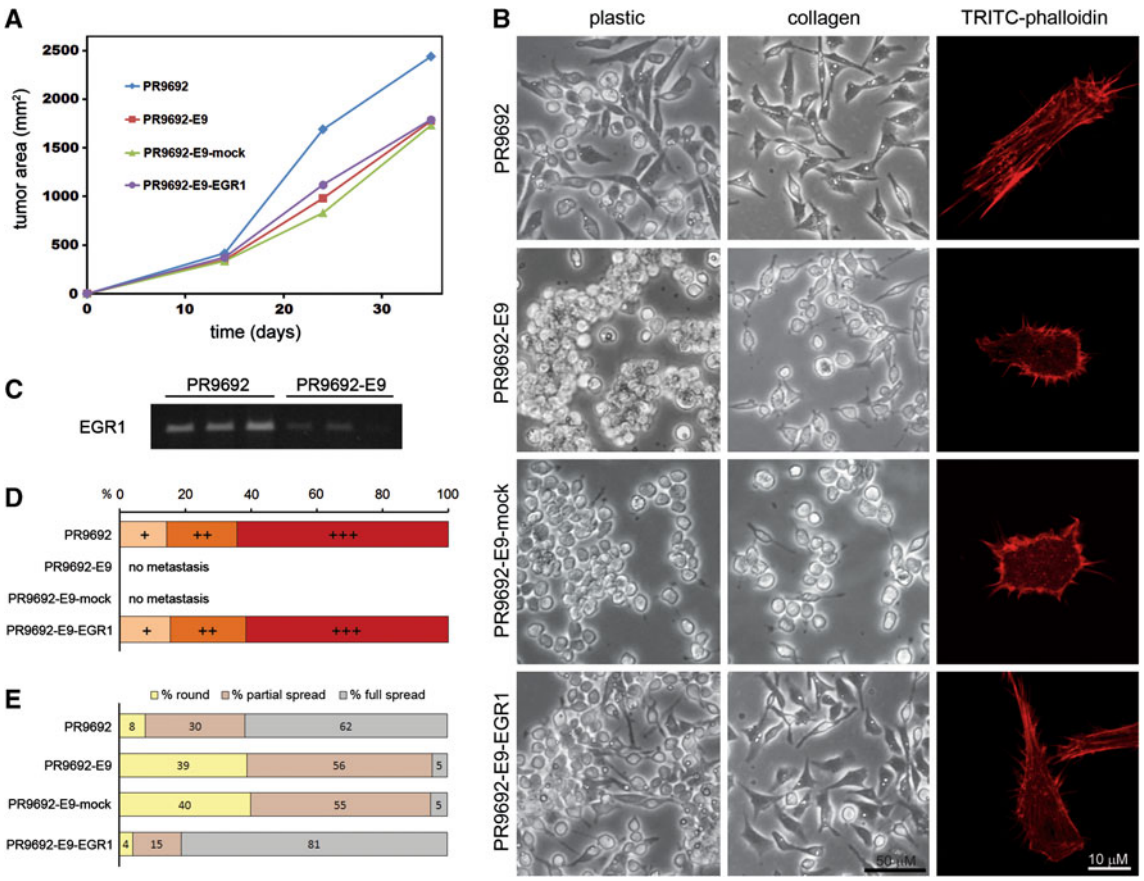

Fig. 1 **a** Growth kinetics of primary tumors formed by PR9692 and derived cell lines. The area of primary tumors was measured over the course of 35 days post-inoculation; average values of six animals in each group are plotted against time. **b** Typical appearance of living cells cultured on uncoated plastic and type I collagen-coated surfaces. TRITC-falloidin—fluorescently stained actin in fixed cells cultured on type I collagen-coated surfaces. **c** EGR1 mRNA levels in cultured cells detected by RT-PCR (see Fig. 2c for the corresponding GAPDH control). **d** Number and size of metastases assessed in animals 5 weeks after inoculation of cells. The extent of lung metastasis: +, multiple (>10) small and 1–3 medium sized (3–4 mm) metastases; ++, multiple small and more than 3 medium sized metastases and/or 1–3 large (4–5 mm) isolated metastases; +++, lungs overgrown with medium to large metastases growing together, frequently more than 50% of lungs formed by tumor tissue, in some chicks metastases seized majority of the lungs. **e** Adhesive behavior of PR9692 and derived cells grown on type I collagen coated surfaces was inspected in microphotographs and cell populations were divided into three categories: round cells (sticking to the surface), partially spread cells with some protrusions, but still rounded middle part and fully spread flat cells

to participate in processes related to metastatic spreading of tumor cells. These include cell adhesion (ITGA4, ITGA11, NCAM1), motility (MYL9) and ECM degradation (PCSK6). Notably, there are also striking differences in genes participating in ECM production (e.g., HAS2, COL1A2, all three type VI collagens). It is well known that changes in mRNA levels can generally be caused by several mechanisms including the action of transcription factor(s), promoter methylation/demethylation, gene mutation, as well as by postranscriptional mechanisms like RNA interference or mRNA stability regulation by protein factors. We further focused on the possible involvement of transcription factors. Careful assessment of our gene expression data revealed the transcription factor EGR1 was downregulated (20-fold in microarray, approximately threefold in qPCR analysis) in non-metastasizing cells, suggesting it might be important for metastasis (see Fig. 1c for RT-PCR comparison of mRNA levels in three independent samples of each cell line). This hypothesis was further supported by the well described role of EGR1 as an effector of several signaling pathways, including the TGFβ cascade [13, 15] that is known to be important for the metastatic progression of various tumor types. Moreover, previous literature has demonstrated that high expression of EGR1 positively correlates with the metastatic potential of gastric carcinomas [28] and the expression of the closely related gene, EGR3 regulates the invasive behavior of breast carcinoma [29]. Based on these observations, we wondered whether increasing EGR1 expression in PR9692-E9 cells could restore their metastatic potential.

Generation of PR9692-E9-EGR1 cells

To increase the expression of EGR1 in PR9692-E9 cells, we transfected KUNDRA packaging cells with the SFCV-LE retroviral vector encoding chicken EGR1 tagged N-terminally with a myc-tag and G418 resistance gene (SFCV-ME-EGR1). The resulting replication-defective virus was subsequently used to infect PR9692-E9 cells and G418 resistant cell clones were pooled and maintained in culture for several passages before in vivo experiments.

Table 1 Selected genes differentially expressed in PR9692 and PR9692-E9 cells

Gene symbol	Gene title	Log_2 change
Upregulated in PR9692-E9 compared to PR9692		
CACNA2D1	Calcium channel, voltage-dependent, alpha 2/delta subunit 1	6.1
LIPI	Lipase, member I	5.9
FABP1	Fatty acid binding protein 1, liver	5.2
EYA2	Eyes absent homolog 2	5.1
SLITRK6	SLIT and NTRK-like family, member 6	4.7
SCN2A	Sodium channel, voltage-gated, type II, alpha 2	4.6
IRX1	Iroquois homeobox 1	4.4
NMU	Neuromedin U	4.4
SEPP1	Selenoprotein P, plasma, 1	4.4
CADM1	Cell adhesion molecule 1	4.0
AQP9	Aquaporin 9	3.9
CPEB1	Cytoplasmic polyadenylation element binding protein 1	3.8
FGFBP1	Fibroblast growth factor binding protein 1	3.8
ARHGAP12	Rho GTPase-activating protein 12	3.7
PTGER4	Prostaglandin E receptor 4 (subtype EP4)	3.7
TSPAN7	Tetraspanin 7	3.4
RICS	Rho GTPase-activating protein RICS	3.3
CTSD	Cathepsin D	3.2
CD36	Thrombospondin receptor CD36	3.2
SFRP4	Secreted frizzled-related protein 4	2.9
Downregulated in PR9692-E9 compared to PR9692		
COL6A3	Collagen, type VI, alpha 3	−10.4
COL5A1	Collagen, type V, alpha 1	−8.8
COL6A2	Collagen, type VI, alpha 2	−8.3
ITGA4	Integrin, alpha 4	−8.1
COL1A2	Collagen, type I, alpha 2	−7.3
COL6A1	Collagen, type VI, alpha 1	−7.3
RARRES2	Retinoic acid receptor responder (tazarotene induced) 2	−6.8
MGAT3	Mannosyl (beta-1,4-)-glycoprotein beta-1,4-N-acetylglucosaminyltransferase	−6.5
NCAM1	Neural cell adhesion molecule 1	−5.7
ITGA11	Integrin, alpha 11	−5.6
PCSK6	Proprotein convertase subtilisin/kexin type 6	−5.5
PRKCH	Protein kinase C, eta	−5.2
MYL9	Myosin, light chain 9, regulatory	−5.1
CMTM7	CKLF-like MARVEL transmembrane domain containing 7	−4.7
AQP1	Aquaporin 1	−4.6
EGR1	Early growth response 1	−4.3
HAS2	Hyaluronan synthase 2	−4.1
MSRB3	Methionine sulfoxide reductase B3	−3.9
CBY1	Chibby homolog 1	−3.6
LASS6	LAG1 homolog, ceramide synthase 6	−3.5

The resulting PR9692-E9-EGR1 cells were screened for the presence of myc-tagged EGR1 (ME-EGR1) by immunoblotting (Fig. 2d). Control cells infected with empty SFCV-LE retroviral vector (PR9692-E9-mock) were prepared in the same fashion.

Metastatic behavior of PR9692-E9-EGR1 cells

Animals injected with PR9692, PR9692-E9, PR9692-E9-mock, or PR9692-E9-EGR1 cells were killed 5 weeks post-injection and their lungs inspected for the presence of metastases. High-grade metastatic spreading was detected in all animals injected with either PR9692 or PR9692-E9-EGR1 cells while no significant metastasis was detected in animals injected with PR9692-E9 or PR9692-E9-mock cells. Importantly, the size and number of metastatic foci in animals injected with PR9692-E9-EGR1 were comparable to those induced by PR9692 cells (Fig. 1d).

Adhesion properties, actin cytoskeleton characteristics, and migratory behavior of metastatic and non-metastatic PR9692-derived cells

Analysis of the morphology of PR9692-E9-EGR1 cells revealed that they not only exhibit identical metastatic behavior to PR9692 cells but also assume a similar morphology on collagen-coated cell culture plastic (Fig. 1b) and adhere to uncoated plastic with some of them able to spread. In contrast, the non-metastatic PR9692-E9 and PR9692-E9-mock cells were only able to adhere to surfaces coated with collagen or fibronectin. To investigate in more detail the adhesive behavior of each cell line, we compared the morphology and degree of cell spreading on type I collagen-coated plates. Microimages of each cell population were inspected and cells divided into three categories depending on the degree of spreading: not spread (round shaped), partially spread (rounded with

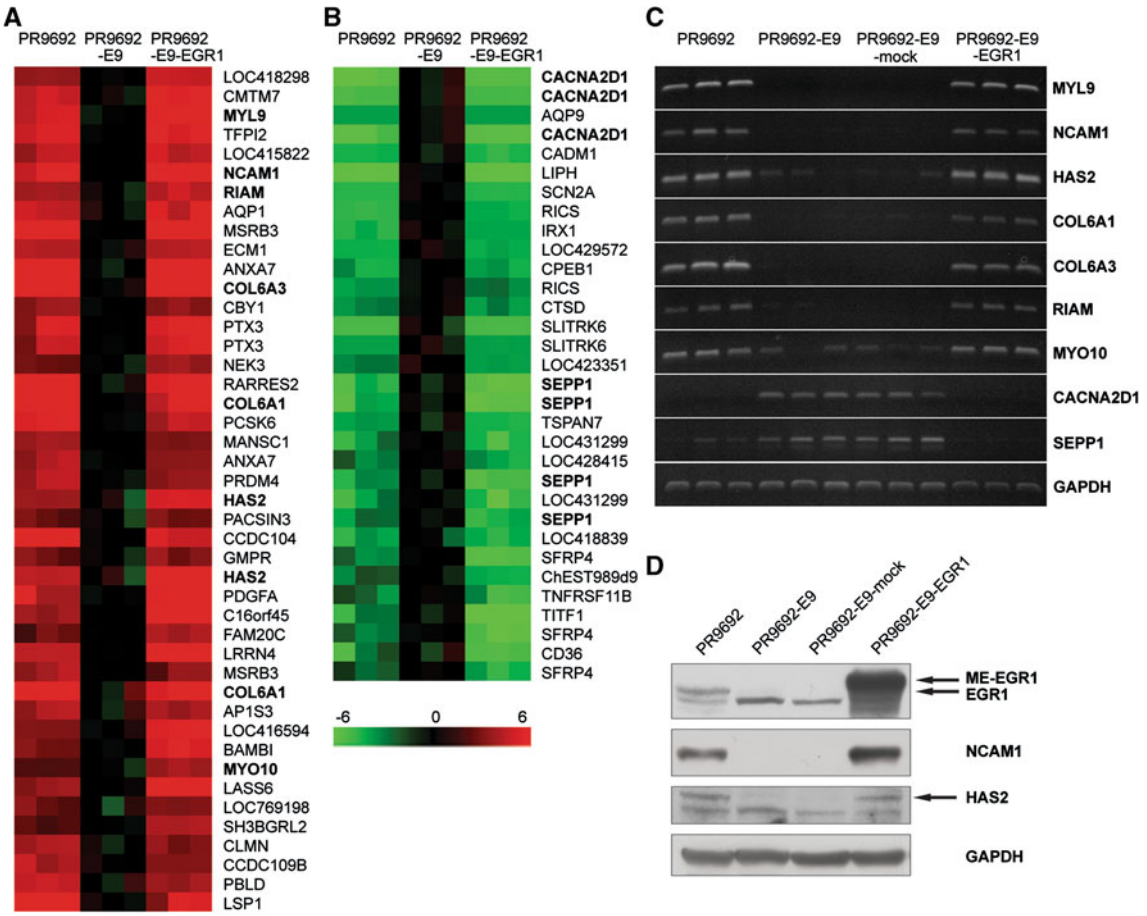

Fig. 2 Genes associated with metastatic phenotype. Gene clustering analysis was performed using the QT_Clust algorithm. **a** Gene clusters containing genes with a high expression in metastatic PR9692 and PR9692-E9-EGR1 cells but low expression in non-metastatic PR9692-E9 cells. **b** Genes with a lowered expression in metastatic compared with non-metastatic cells. The multiple presence of some genes in the list is a consequence of a probe set redundancy of the microarray. Genes further analyzed by PCR and qPCR are shown in *boldface*. **c** PCR analysis of differential gene expression. cDNA samples obtained from three independent cell cultures of each cell line PCR amplified with oligonucleotide primers for selected genes and resolved on an agarose gel. **d** Protein levels corresponding to selected differentially expressed genes were analyzed by Western blotting. *ME-EGR1* stands for c-myc epitope-labeled EGR1

narrow protrusions), and fully spread (flat elongated or stellate cells) (Fig. 1e). While both metastatic cell lines exhibited a high tendency to spread on the collagen-coated surface, the majority of non-metastatic PR9692-E9 and PR9692-E9-mock cells, though adhered to the plate, remained rounded. To visualize differences in the organization of the actin cytoskeleton in the metastatic and non-metastatic cells adhered to collagen, cells were stained with TRITC-phalloidin. Substantial differences were revealed, particularly in the ability to assume cell polarity and to form stress fibers. Some differences were also noted in the appearance of filopodia. While both metastatic cell lines assume polarized morphology with distinct stress fibers and long thin filopodia are observed in a subpopulation of the cells, non-metastatic PR9692-E9 and PR9692-E9-mock cells typically show unpolarized rounded morphology with actin-rich membrane ruffles and fewer short thick filopodia (Fig. 1b and Supplementary Fig. S2). To find out whether the differing adhesion abilities of the cells are also accompanied by differences in in vitro migratory behavior, the time-lapse microscopy was performed and video sequences were created, each representing approximately 24 h of cell culture (Supplementary Movies SM1 through SM4 available at http://www.img.cas.cz/mv/supplements). Visual comparison of the movies revealed that subpopulations of PR9692 and PR9692-E9-EGR1 cells perform the typical mesenchymal locomotion with easily discernible front end lamellipodium and rear end uropod which is being retracted during the motion. In contrast, although subpopulations of PR9696-E9 and PR9692-E9-mock cells show full adhesion to the collagen coated surface and are able to stick out and retract protrusions, their motion seems to be performed in a different way, is rather defective and the front-rear polarity cannot be observed in these cells.

Gene expression analysis of PR9692-E9-EGR1 cells

To identify potential EGR1 target genes involved in regulating metastatic spreading, we analyzed PR9692-E9-EGR1 cells by microarray analysis. The resulting gene expression profile was then compared to the gene expression data obtained previously from the PR9692 and PR9692-E9 cells. A selection of genes with the most significant changes is listed in Table 2 with a complete list of all affected genes presented in Supplementary Table S2. The comparison revealed that the exogenous expression of EGR1 in the non-metastatic cell line reconstituted the expression of a number of genes to levels comparable to the parental PR9692 metastatic cells. We also observed genes whose expression differed in the PR9692 and PR9692-E9 cells and remained unaffected by exogenous EGR1 expression. Finally, we also identified genes not activated in parental cells but expressed in the EGR1 reconstituted PR9692-E9-EGR1 cells. The fact that some genes are activated in the EGR1 reconstituted cells and not in parental cells (e.g., RBM24) may result from the increased level of EGR1 expression in PR9692-E9-EGR1 cells relative to the endogenous levels detected in PR9692 cells.

As the genes that show similar expression in both metastatic cell lines (PR9692 and PR9692-E9-EGR1) and are either downregulated or upregulated in the non-metastatic cells (PR9692-E9) are supposed to be involved in a presumptive metastatic transcription program, the identification of such genes among all affected genes is the most crucial point of our work. To identify these genes, we performed cluster analysis in the MeV software environment [26] using quasi-two-color chip representation of data (with median of PR9692-E9 as a reference value) and QT_Clust algorithm [27] as these settings provided the most satisfactory results (Fig. 2a, b and Supplementary Table S3). For the further PCR and qPCR verification of gene expression differences, we chose several genes from both relevant clusters (Fig. 2a, b genes in bold). The results of PCR analysis are presented in Fig. 2c. For qPCR, RNA samples used for microarray analysis (cells cultured on uncoated plastic) as well as independent RNAs isolated from cells cultured on collagen-coated surface were used to check if the expression of the genes was not influenced by adhesive conditions. The qPCR data correlated well with the microarrays (Supplementary Fig. S3) and although the absolute expression level of some of the genes was affected by the collagen coating, the relative differences did not significantly differ from the "bare plastic" samples. To further confirm the microarray and PCR results, protein levels of NCAM1 and HAS2 were assayed in immunoblotting experiments. Expression level differences similar to those revealed on mRNA level were observed providing additional proof of biological relevance of the microarray data (Fig. 2d).

The list of genes showing similar expression in PR9692 and PR9692-E9-EGR1 and downregulation in PR9692-E9 contains known important regulators of tumor metastasis, genes that have not been correlated with metastatic behavior so far, as well as genes of unknown function. MYL9 gene encodes myosin regulatory light chain (MRLC/MLC/MLC2), a target of regulatory phosphorylation by the myosin light chain kinase (MLCK) and Rho-kinase (ROCK) [30]. This phosphorylation drives actin cytoskeleton contractions and is important for adhesion maturation, establishment of polarity, and subsequent migration of the cells [31, 32]. MLC is an essential regulator of all processes requiring a generation of mechanical force by actin cytoskeleton. Recently, an alternative to the classical mesenchymal mode of cancer cell migration in the three-dimensional environment was demonstrated. This

Table 2 Selected genes differentially expressed in PR9692-E9-EGR1 and PR9692-E9 cells

Gene symbol	Gene title	Log_2 change
Upregulated in PR9692-E9-EGR1 compared to PR9692-E9		
RBM24	RNA binding motif protein 24	10.5
COL6A3	Collagen, type VI, alpha 3	9.0
PDGFA	Platelet-derived growth factor alpha polypeptide	6.8
HAS2	Hyaluronan synthase 2	6.7
SERPINB2	Serpin peptidase inhibitor, clade B (ovalbumin), member 2	6.3
MYL9	Myosin, light chain 9, regulatory	6.3
COL6A1	Collagen, type VI, alpha 1	6.3
NCAM1	Neural cell adhesion molecule 1	6.2
INHBA	Inhibin, beta A	6.1
SERPINB10	Serpin peptidase inhibitor, clade B (ovalbumin), member 10	6.0
CMTM7	CKLF-like MARVEL transmembrane domain containing 7	5.9
RARRES2	Retinoic acid receptor responder (tazarotene induced) 2	5.7
TFPI2	Tissue factor pathway inhibitor 2	5.5
BAMBI	BMP and activin membrane-bound inhibitor homolog	5.4
RDH10	Retinol dehydrogenase 10 (all-trans)	5.1
AQP1	Aquaporin 1	5.1
CCDC104	Coiled-coil domain containing 104	4.8
TAGLN	Transgelin	4.5
LSP1	Lymphocyte-specific protein 1	4.4
PCSK6	Proprotein convertase subtilisin/kexin type 6	4.4
Downregulated in PR9692-E9-EGR1 compared to PR9692-E9		
ALDOB	Aldolase B, fructose-bisphosphate	−7.2
CALML4	Calmodulin-like 4	−6.9
TMEM26	Transmembrane protein 26	−6.8
NKX2-1	NK2 homeobox 1	−6.5
KLF15	Kruppel-like factor 15	−6.3
LIPI	Lipase, member I	−5.9
ARHGDIB	Rho GDP dissociation inhibitor (GDI) beta	−5.9
CACNA2D1	Calcium channel, voltage-dependent, alpha 2/delta subunit 1	−5.9
SFRP4	Secreted frizzled-related protein 4	−5.7
SEPP1	Selenoprotein P, plasma, 1	−5.7
RASGRP3	RAS guanyl releasing protein 3 (calcium and DAG-regulated)	−5.5
CD36	Thrombospondin receptor CD36	−5.3
ZBTB16	Zinc finger and BTB domain containing 16	−5.3
SLITRK6	SLIT and NTRK-like family, member 6	−4.7
TNFRSF11B	Tumor necrosis factor receptor superfamily, member 11b (osteoprotegerin)	−4.5
CADM1	Cell adhesion molecule 1	−4.2
TTC8	Tetratricopeptide repeat domain 8	−4.2
TSPAN7	Tetraspanin 7	−4.0
IRX1	Iroquois homeobox 1	−4.0
RAB30	RAB30, RAS oncogene family	−4.0

mode of migration, termed amoeboid, does not require the use of proteolytic enzymes to invade the ECM and instead uses the force generated by acto-myosin contractions [33, 34]. The amoeboid mode of migration can either be activated by specific conditions or be the default mode in some cancer cells [35]. Importantly, MLC is indispensable for both types of cancer cell migration. The RIAM gene encodes an adaptor protein that mediates Rap1-induced cell adhesion [36]. It was recently demonstrated that RIAM activates integrins by bringing talin to plasma membrane [37]. The MYO10 gene's

product myosin X is a critical component of the apparatus responsible for creating filopodia [38–40]. These narrow hair-like protrusions of actin cytoskeleton are important for cellular adhesion to substratum and subsequent migration [41]. Proprotein convertase subtilisin/kexin 6 (PCSK6 alias PACE4), a processing protease closely related to furin, proteolytically activates MMP3, MT1-MMP, and various other substrates involved in tumor progression [42], and was shown to increase the invasive ability of carcinomas [43]. NCAM1 (alias NCAM or CD56) was originally believed to be involved in mediating tumor cell adhesion to the endothelium. However, a recent paper has revealed a more direct involvement of this molecule in focal adhesion assembly, cell spreading, and invasive behavior [44, 45]. The hyaluronan synthase 2, encoded by HAS2 gene, is an enzyme responsible for the production of hyaluronan, an important polysaccharide component of ECM produced by fibroblasts and other mesenchymal cells. The involvement of hyaluronan production by cancer cells in their invasive behavior was demonstrated by several reports [46–48]. Interestingly, type VI collagen, which consists of three peptides encoded by COL6A1, COL6A2, and COL6A3 genes, was suggested to cooperate with hyaluronan in the formation of a tumor microenvironment that supports specific angiogenesis forming vascular networks to promote cancer dissemination in melanomas [49].

Discussion

Transcriptional control of metastatic behavior has been extensively studied in transformed epithelial cells. The transcription factors identified there to play important roles in the metastatic spreading are in almost all cases basic regulators of mesenchymal phenotype establishment and maintenance (twist, ZEB1, ZEB2, snail, slug, TCF3) [50, 51]. Although transformed mesenchymal cells express these transcription factors not all mesenchymal tumors metastasize. This phenomenon suggests the existence of an additional level of transcriptional regulation to control genes important for metastatic dissemination. Given the complexity of the metastatic process, the genes controlled by such regulation may be important for various activities including cellular motility, ECM degradation, survival in circulation, adhesion to endothelium, and invasion of distant tissues.

The genes identified in this study to be regulated by EGR1 play important roles in a variety of processes that are obligatory for the cells to be metastatic. Probably the most intriguing potential EGR1 target revealed here is the MYL9 gene as its expression endows cells with the ability to perform acto-myosin contractions in response to adhesive signaling. This ability is a pre-requisite for all types of cellular motility in cancer cells. Recently, the expression of MYL9 gene was shown to be controlled by MRTF-SRF complex in human breast carcinoma and mouse melanoma cell lines [52]. It is known that the transcription factor SRF, in cooperation with myocardin family coactivators, regulates the expression of actin cytoskeleton contractility related genes in smooth muscle cells and myofibroblasts [53]. In PR9692 and derived cells, however, the majority of these genes are not significantly expressed (data not shown). Based on this observation, we believe that in cancer cells, EGR1 might regulate the expression of MYL9 independently of SRF and thus be an alternate activator obviating the Rho-actin-MRTF-SRF pathway in cancer cells. Analysis of the promoter region of MYL9 gene in the chicken, human, and mouse genomes indeed reveals the presence of canonical EGR1 binding sites (GMGGGGGCG) (data not shown).

Previous attempts to elucidate and characterize metastasis-associated genes have utilized metastatic and non-metastatic cell lines derived from the same type of tumor to compare gene expression profiles. Only rarely, however, have researchers used cell lines of a single clonal origin to ensure no difficulties in interpreting the resulting data due to background differences. In contrast to some of the previous studies, particularly those carried out on inherently heterogenous tumor samples or cell lines of different origin, our work revealed metastatic potential-related differential expression of genes that have clear mechanistic connection to the process. This validates the PR9692 cell lines model as a useful tool to study the biological background of tumor metastasis.

Acknowledgments We thank Dr. Alicia Corlett for the help with manuscript preparation, Dr. Robert Ivánek for the help with microarray analysis, and Dr. Michal Kolář for an expert advice on the statistical processing of qPCR data. This work was supported by grants AV0Z50520514 and KAN200520801 from GAAVCR and LC06061 from MEYS to M.D. and 204/07/1030 from GACR to J.P.

References

1. Deryugina EI, Quigley JP (2006) Matrix metalloproteinases and tumor metastasis. Cancer Metastasis Rev 25:9–34
2. Olson MF, Sahai E (2009) The actin cytoskeleton in cancer cell motility. Clin Exp Metastasis 26:273–287
3. Brooks SA, Lomax-Browne HJ, Carter TM, Kinch CE, Hall DM (2010) Molecular interactions in cancer cell metastasis. Acta Histochem 112:3–25
4. Yokota J (2000) Tumor progression and metastasis. Carcinogenesis 21:497–503
5. Yilmaz M, Christofori G (2009) EMT, the cytoskeleton, and cancer cell invasion. Cancer Metastasis Rev 28:15–33
6. Scheel C, Onder T, Karnoub A, Weinberg RA (2007) Adaptation versus selection: the origins of metastatic behavior. Cancer Res 67:11476–11479 (discussion 11479-80)

7. Gadd MA, Casper ES, Woodruff JM, McCormack PM, Brennan MF (1993) Development and treatment of pulmonary metastases in adult patients with extremity soft tissue sarcoma. Ann Surg 218:705–712
8. Songur N, Dinc M, Ozdilekcan C, Eke S, Ok U, Oz M (2003) Analysis of lung metastases in patients with primary extremity sarcoma. Sarcoma 7:63–67
9. Tournay O, Benezra R (1996) Transcription of the dominant-negative helix-loop-helix protein Id1 is regulated by a protein complex containing the immediate-early response gene Egr-1. Mol Cell Biol 16:2418–2430
10. Zhu X, Lin Y, Bacanamwo M, Chang L, Chai R, Massud I, Zhang J, Garcia-Barrio MT, Thompson WE, Chen YE (2007) Interleukin-1 beta-induced Id2 gene expression is mediated by Egr-1 in vascular smooth muscle cells. Cardiovasc Res 76:141–148
11. Shingu T, Bornstein P (1994) Overlapping Egr-1 and Sp1 sites function in the regulation of transcription of the mouse thrombospondin 1 gene. J Biol Chem 269:32551–32557
12. Copertino DW, Edelman GM, Jones FS (1997) Multiple promoter elements differentially regulate the expression of the mouse tenascin gene. Proc Natl Acad Sci USA 94:1846–1851
13. Chen SJ, Ning H, Ishida W, Sodin-Semrl S, Takagawa S, Mori Y, Varga J (2006) The early-immediate gene EGR-1 is induced by transforming growth factor-beta and mediates stimulation of collagen gene expression. J Biol Chem 281:21183–21197
14. Silverman ES, Khachigian LM, Lindner V, Williams AJ, Collins T (1997) Inducible PDGF A-chain transcription in smooth muscle cells is mediated by Egr-1 displacement of Sp1 and Sp3. Am J Physiol 273:H1415–H1426
15. Bhattacharyya S, Ishida W, Wu M, Wilkes M, Mori Y, Hinchcliff M, Leof E, Varga J (2009) A non-Smad mechanism of fibroblast activation by transforming growth factor-beta via c-Abl and Egr-1: selective modulation by imatinib mesylate. Oncogene 28:1285–1297
16. Padua D, Massague J (2009) Roles of TGFbeta in metastasis. Cell Res 19:89–102
17. Svoboda J, Dvorak M, Guntaka R, Geryk J (1986) Transmission of (LTR, v-src, LTR) without recombination with a helper virus. Virology 153:314–317
18. Fuerstenberg SM, Vennstrom B (1993) Versatile avian retrovirus vectors. Anal Biochem 209:375–376
19. Plachy J, Vilhelmova M (1984) Syngeneic lines of chickens. VII. The lines derived from the recombinants at the B complex (MHC) of Rous sarcoma regressor and progressor inbred lines of chickens. Folia Biol (Praha) 30:189–201
20. Svoboda J, Plachy J, Hejnar J, Karakoz I, Guntaka RV, Geryk J (1992) Tumor induction by the LTR, v-src, LTR DNA in four B (MHC) congenic lines of chickens. Immunogenetics 35:309–315
21. Cosset FL, Legras C, Chebloune Y, Savatier P, Thoraval P, Thomas JL, Samarut J, Nigon VM, Verdier G (1990) A new avian leukosis virus-based packaging cell line that uses two separate transcomplementing helper genomes. J Virol 64:1070–1078
22. Irizarry RA, Bolstad BM, Collin F, Cope LM, Hobbs B, Speed TP (2003) Summaries of Affymetrix GeneChip probe level data. Nucleic Acids Res 31:e15
23. Smyth GK (2004) Linear models and empirical Bayes methods for assessing differential expression in microarray experiments. Stat Appl Genet Mol Biol 3, Article 3
24. Gentleman RC, Carey VJ, Bates DM, Bolstad B, Dettling M, Dudoit S, Ellis B, Gautier L, Ge Y, Gentry J, Hornik K, Hothorn T, Huber W, Iacus S, Irizarry R, Leisch F, Li C, Maechler M, Rossini AJ, Sawitzki G, Smith C, Smyth G, Tierney L, Yang JY, Zhang J (2004) Bioconductor: open software development for computational biology and bioinformatics. Genome Biol 5:R80
25. Benjamini Y, Hochberg Y (1995) Controlling the false discovery rate: a practical and powerful approach to multiple testing. J R Stat Soc B 57:289–300
26. Saeed AI, Sharov V, White J, Li J, Liang W, Bhagabati N, Braisted J, Klapa M, Currier T, Thiagarajan M, Sturn A, Snuffin M, Rezantsev A, Popov D, Ryltsov A, Kostukovich E, Borisovsky I, Liu Z, Vinsavich A, Trush V, Quackenbush J (2003) TM4: a free, open-source system for microarray data management and analysis. Biotechniques 34:374–378
27. Heyer LJ, Kruglyak S, Yooseph S (1999) Exploring expression data: identification and analysis of coexpressed genes. Genome Res 9:1106–1115
28. Kobayashi D, Yamada M, Kamagata C, Kaneko R, Tsuji N, Nakamura M, Yagihashi A, Watanabe N (2002) Overexpression of early growth response-1 as a metastasis-regulatory factor in gastric cancer. Anticancer Res 22:3963–3970
29. Suzuki T, Inoue A, Miki Y, Moriya T, Akahira J, Ishida T, Hirakawa H, Yamaguchi Y, Hayashi S, Sasano H (2007) Early growth responsive gene 3 in human breast carcinoma: a regulator of estrogen-meditated invasion and a potent prognostic factor. Endocr Relat Cancer 14:279–292
30. Totsukawa G, Yamakita Y, Yamashiro S, Hartshorne DJ, Sasaki Y, Matsumura F (2000) Distinct roles of ROCK (Rho-kinase) and MLCK in spatial regulation of MLC phosphorylation for assembly of stress fibers and focal adhesions in 3T3 fibroblasts. J Cell Biol 150:797–806
31. Gutjahr MC, Rossy J, Niggli V (2005) Role of Rho, Rac, and Rho-kinase in phosphorylation of myosin light chain, development of polarity, and spontaneous migration of Walker 256 carcinosarcoma cells. Exp Cell Res 308:422–438
32. Vicente-Manzanares M, Koach MA, Whitmore L, Lamers ML, Horwitz AF (2008) Segregation and activation of myosin IIB creates a rear in migrating cells. J Cell Biol 183:543–554
33. Wolf K, Mazo I, Leung H, Engelke K, von Andrian UH, Deryugina EI, Strongin AY, Bröcker EB, Friedl P (2003) Compensation mechanism in tumor cell migration: mesenchymal-amoeboid transition after blocking of pericellular proteolysis. J Cell Biol 160:267–277
34. Sahai E, Marshall CJ (2003) Differing modes of tumour cell invasion have distinct requirements for Rho/ROCK signalling and extracellular proteolysis. Nat Cell Biol 5:711–719
35. Rosel D, Brábek J, Tolde O, Mierke CT, Zitterbart DP, Raupach C, Bicanová K, Kollmannsberger P, Panková D, Vesely P, Folk P, Fabrym B (2008) Up-regulation of Rho/ROCK signaling in sarcoma cells drives invasion and increased generation of protrusive forces. Mol Cancer Res 6:1410–1420
36. Lafuente EM, van Puijenbroek AA, Krause M, Carman CV, Freeman GJ, Berezovskaya A, Constantine E, Springer TA, Gertler FB, Boussiotis VA (2004) RIAM, an Ena/VASP and profilin ligand, interacts with Rap1-GTP and mediates Rap1-induced adhesion. Dev Cell 7:585–595
37. Lee HS, Lim CJ, Puzon-McLaughlin W, Shattil SJ, Ginsberg MH (2009) RIAM activates integrins by linking talin to ras GTPase membrane-targeting sequences. J Biol Chem 284:5119–5127
38. Berg JS, Cheney RE (2002) Myosin-X is an unconventional myosin that undergoes intrafilopodial motility. Nat Cell Biol 4:246–250
39. Tokuo H, Ikebe M (2004) Myosin X transports Mena/VASP to the tip of filopodia. Biochem Biophys Res Commun 319:214–220
40. Bohil AB, Robertson BW, Cheney RE (2006) Myosin-X is a molecular motor that functions in filopodia formation. Proc Natl Acad Sci USA 103:12411–12416
41. Mattila PK, Lappalainen P (2008) Filopodia: molecular architecture and cellular functions. Nat Rev Mol Cell Biol 9:446–454

42. Bassi DE, Mahloogi H, Klein-Szanto AJ (2000) The proprotein convertases furin and PACE4 play a significant role in tumor progression. Mol Carcinog 28:63–69
43. Hubbard FC, Goodrow TL, Liu SC, Brilliant MH, Basset P, Mains RE, Klein-Szanto AJ (1997) Expression of PACE4 in chemically induced carcinomas is associated with spindle cell tumor conversion and increased invasive ability. Cancer Res 57:5226–5231
44. Zocchi MR, Vidal M, Poggi A (1993) Involvement of CD56/N-CAM molecule in the adhesion of human solid tumor cell lines to endothelial cells. Exp Cell Res 204:130–135
45. Lehembre F, Yilmaz M, Wicki A, Schomber T, Strittmatter K, Ziegler D, Kren A, Went P, Derksen PW, Berns A, Jonkers J, Christofori G (2008) NCAM-induced focal adhesion assembly: a functional switch upon loss of E-cadherin. EMBO J 27:2603–2615
46. Simpson MA, Wilson CM, Furcht LT, Spicer AP, Oegema TR Jr, McCarthy JB (2002) Manipulation of hyaluronan synthase expression in prostate adenocarcinoma cells alters pericellular matrix retention and adhesion to bone marrow endothelial cells. J Biol Chem 277:10050–10057
47. Udabage L, Brownlee GR, Waltham M, Blick T, Walker EC, Heldin P, Nilsson SK, Thompson EW, Brown TJ (2005) Antisense-mediated suppression of hyaluronan synthase 2 inhibits the tumorigenesis and progression of breast cancer. Cancer Res 65:6139–6150
48. Cook AC, Chambers AF, Turley EA, Tuck AB (2006) Osteopontin induction of hyaluronan synthase 2 expression promotes breast cancer malignancy. J Biol Chem 281:24381–24389
49. Daniels KJ, Boldt HC, Martin JA, Gardner LM, Meyer M, Folberg R (1996) Expression of type VI collagen in uveal melanoma: its role in pattern formation and tumor progression. Lab Invest 75:55–66
50. Yang J, Mani SA, Donaher JL, Ramaswamy S, Itzykson RA, Come C, Savagner P, Gitelman I, Richardson A, Weinberg RA (2004) Twist, a master regulator of morphogenesis, plays an essential role in tumor metastasis. Cell 117:927–939
51. Peinado H, Olmeda D, Cano A (2007) Snail, Zeb and bHLH factors in tumour progression: an alliance against the epithelial phenotype? Nat Rev Cancer 7:415–428
52. Medjkane S, Perez-Sanchez C, Gaggioli C, Sahai E, Treisman R (2009) Myocardin-related transcription factors and SRF are required for cytoskeletal dynamics and experimental metastasis. Nat Cell Biol 11:257–268
53. Miano JM, Long X, Fujiwara K (2007) Serum response factor: master regulator of the actin cytoskeleton and contractile apparatus. Am J Physiol Cell Physiol 292:C70–C81